Reconstructions of Noisy Digital Contours with Maximal Primitives Based on Multi-scale/Irregular Geometric Representation and Generalized Linear Programming

Antoine Vacavant[1(✉)], Bertrand Kerautret[2], Tristan Roussillon[3], and Fabien Feschet[1]

[1] Université Clermont Auvergne, CNRS, SIGMA Clermont, Institut Pascal, 63000 Clermont-Ferrand, France
{antoine.vacavant,fabien.feschet}@uca.fr
[2] LORIA, UMR CNRS 7503, Université de Lorraine, 54506 Vandœuvre-lès-Nancy, France
bertrand.kerautret@univ-lorraine.fr
[3] Univ Lyon, INSA-LYON, LIRIS UMR 5205, 69622 Villeurbanne, France
tristan.roussillon@liris.cnrs.fr

Abstract. The reconstruction of noisy digital shapes is a complex question and a lot of contributions have been proposed to address this problem, including blurred segment decomposition or adaptive tangential covering for instance. In this article, we propose a novel approach combining multi-scale and irregular isothetic representations of the input contour, as an extension of a previous work [Vacavant et al., A Combined Multi-Scale/Irregular Algorithm for the Vectorization of Noisy Digital Contours, CVIU 2013]. Our new algorithm improves the representation of the contour by 1-D intervals, and achieves afterwards the decomposition of the contour into maximal arcs or segments. Our experiments with synthetic and real images show that our contribution can be employed as a relevant option for noisy shape reconstruction.

Keywords: Digital shape analysis · Irregular isothetic grids · Multi-scale analysis · Decomposition into maximal arcs · Decomposition into maximal segments

1 Introduction

The representation of digital contours is an important task in image analysis applications, since binary shapes obtained by image processing algorithms (preprocessing and segmentation) may be altered by noise. A lot of efforts have been made on these algorithms to produce *smooth contours*, by developing sophisticated deblurring and denoising algorithms [14], or by integrating regularization

W.G. Kropatsch et al. (Eds.): DGCI 2017, LNCS 10502, pp. 291–303, 2017.
DOI: 10.1007/978-3-319-66272-5_24

terms in segmentation process for instance [26]. However, these approaches significantly raise the computational complexity of the complete image analysis pipeline, and include other input-noise-dependent parameters to be tediously set for any new specific applications.

Hence, another approach consists in obtaining a faithful geometrical representation directly from any noisy digital contours. A lot of research works have addressed this question by *fitting parametric curves* (*e.g.* B-splines, rational Gaussian curves) to the input points [4,8,10]. These approaches require a parameter depending on input noise scale, in order to fit the objective function at best. In general, they do not use the fact that digital points belong to $\mathbb{Z}^2$, as this is always the case in the image plane.

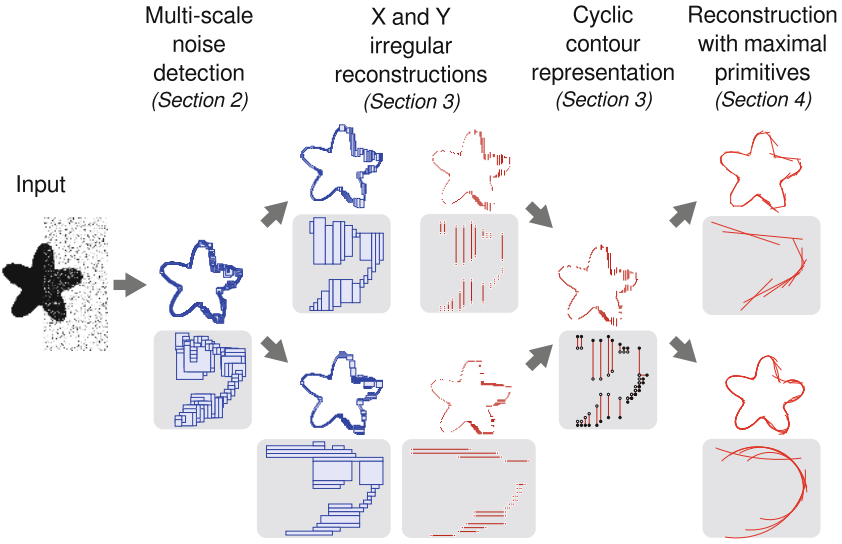

Fig. 1. Global pipeline of our approach. Input: a noisy contour. Output: maximal geometric primitives. Stages are: 1- Extraction of a multi-scale representation (unsupervised geometric noise detector); 2- Irregular isothetic representation (non overlapping cells) in X and Y directions; 3- 1-D intervals representation; 4- Fusion of the two directions to achieve a faithful geometric structure of the input contour.

In the digital geometry community, an important literature has been dedicated to this problem since the 80's, by representing contours with several kinds of primitives (segments, arcs of circle). Thanks to theoretical concepts designed in digital geometry, these approaches extend the scheme of *vectorization*, well-known in document analysis [3], consisting in converting pixels to line segments. In particular, some publications tackle the issue of fitting both straight segments and circular arcs to digital contours at the same time. The famous approach of Rosin and West [18] relies on least square fitting and is non parametric. Another parametric technique has been designed by Hilaire and Tombre [9], based on the

notions of fuzzy digital segments and fuzzy digital arcs, and Faure and Feschet [5] by using α-thick decomposition and combinatorial optimization. All of them are robust and accurate whilst the former two suffer from a high time complexity and are restricted to one pixel wide digital curves. Since multi-primitives decomposition can be viewed as a competition between primitives, the complexity can be tackled with an efficient and unified representation of the multiple decompositions with all individuals primitives. Relying on the work of Feschet and Tougne [6], each decomposition can be represented by a circular arc-graph in linear-time. Decomposition into several primitives can be solved in $\mathcal{O}(qn)$ where q is the minimum number of intersecting primitives in the graph [2]. Other recent methods from state-of-the-art opt for different strategies, such as the adaptation of tangential cover [15] or the detection of dominant points [16].

In this article, we propose a novel *unsupervised approach* for reconstructing noisy digital contours by combining multi-scale and irregular isothetic representations as presented in Fig. 1. The complete pipeline of our approach works as follows. From an input (supposedly noisy) closed contour obtained from any image (first column), we first extract a multi-scale object, containing overlapping boxes, with an unsupervised geometric noise detector (second column). We then represent this structure by irregular isothetic objects that is with cells without any overlapping (third column). This is done by following two directions (X and Y axes) simultaneously. Then these two X and Y axis aligned boxes are represented as lists of 1-D intervals between irregular cells (fourth column). Then, we combine both intervals to achieve a faithful geometric structure of the input contour using both X and Y oriented segments (fifth column) in a unified representation of the contour. At the end (sixth column) we compute maximal primitives within this last representation using the same Generalized Linear Programming approach for segments and arcs allowing us to produce decomposition of the contour into maximal straight line segments or circular arcs.

The article is organized as follows. In Sect. 2, we present the first step of our approach, aiming at representing the input contour as a multi-scale set of bounding boxes. These are then analyzed and converted into irregular isothetic structures, exposed in Sect. 3. Then, we describe the way to obtain decompositions into maximal primitives (Sect. 4), and experimental results with real and synthetic contours (Sect. 5) before concluding this article in Sect. 6.

2 Multi-scale Noise Detection

The noise level detection on a digital contour is an important problem, which can influence the quality of geometric estimators or contour representation algorithms. From the digital geometry domain, a method was proposed to automatically detect the amount of noise present on a digital structure [11]. This detection is based on the meaningful scale detection computed from asymptotic properties of the maximal segments. In particular, it is based on a theorem describing the evolution of the lengths of the maximal segments computed on the border of a shape on finer and finer grid sizes [13]. From such a multiscale analysis,

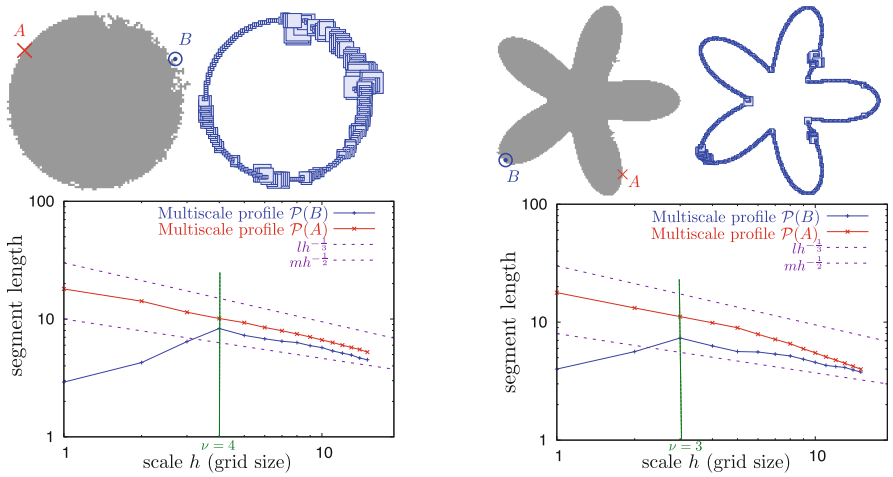

Fig. 2. Conversion of two noisy digital contours into meaningful scales (first row) and illustration of the multiscale profiles for two points A and B (second row)

the proposed algorithm consists in constructing, for each contour points C, a multiscale profile ($\mathcal{P}(C)$) defined by the segment length of all segments covering P for larger and larger grid sizes h (see graph of Fig. 2 second row). From each profile, the noise level is determined by the first scale (nu) minus one for which the slope of $\mathcal{P}$ is decreasing and follows the awaited theoretical bounds between $h^{-\frac{1}{2}}$ and $h^{-\frac{1}{3}}$ if C is on a non null curvature area and near h^{-1} on flat part. On the examples of Fig. 2, the noise levels of points A are 0 since $\mathcal{P}(A)$ is always decreasing and B for the circle (resp. flower) has a noise level of 3 (resp. 3) since $\mathcal{P}(B)$ is increasing until scale 4 (resp. 3). This uncertainty can be represented as boxes and as exposed in Fig. 2 first row, a high noise in the contour will lead to a large box, and *vice-versa*. The algorithm can be tested on-line from any digital contour given by a netizen [12].

3 Irregular Isothetic Cyclic Representation

In this section, we first recall the $\mathbb{I}$-grid (Irregular Isothetic grid) model [22]:

Definition 1 (2-D $\mathbb{I}$-grid). *Let $\mathcal{R}$ be a closed rectangular subset of $\mathbb{R}^2$. A 2-D $\mathbb{I}$-grid G is a tiling of $\mathcal{R}$ with closed rectangular cells whose edges are parallel to the X and Y axes, and whose interiors have a pairwise empty intersection. The position of each cell R is given by its center point $(x_R, y_R) \in \mathbb{R}^2$ and its length along X and Y axes by $(l_R^x, l_R^y) \in {\mathbb{R}_+^*}^2$.*

This model permits to generalize many irregular image representations such as quad-trees, kd-trees, run-length encodings, and the geometry of frames encoded within video coding standards like MPEG, H.264, *etc.* For the rest of the article, we consider the following definitions for $\mathbb{I}$-grids.

Definition 2 (*ve*-**adjacency and** *e*-**adjacency).** *Let R_1 and R_2 be two cells. R_1 and R_2 are ve-adjacent (vertex and edge adjacent) if:*

$$or \begin{cases} |x_{R_1} - x_{R_2}| = \frac{l^x_{R_1}+l^x_{R_2}}{2} \text{ and } |y_{R_1} - y_{R_2}| \leq \frac{l^y_{R_1}+l^y_{R_2}}{2} \\ |y_{R_1} - y_{R_2}| = \frac{l^y_{R_1}+l^y_{R_2}}{2} \text{ and } |x_{R_1} - x_{R_2}| \leq \frac{l^x_{R_1}+l^x_{R_2}}{2} \end{cases}$$

R_1 and R_2 are e-adjacent (edge adjacent) if we consider an exclusive "or" and strict inequalities in the above ve-adjacency definition. The letter k may be interpreted as e or ve in the following definitions.

A k-path from R to R' is a sequence of cells $(R_i)_{1\leq i\leq n}$ with $R = R_1$ and $R' = R_n$ such that for any i, $2 \leq i < n$, R_i is k-adjacent to R_{i-1} and R_{i+1}.

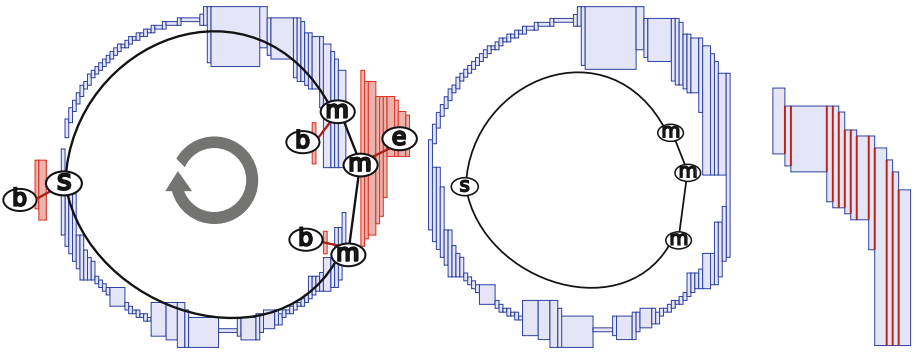

Fig. 3. From the meaningful scales of the *Circle* sample, we reconstruct a set of k-arcs converted to a k-curve thanks to the underlying graph (b). (c) presents a part of the cells obtained with intervals (red) (Color figure online)

Definition 3 (k-**curve).** *Let $A = (R_i)_{1\leq i\leq n}$ be a k-path from R_1 to R_n. Then A is a k-curve iff each cell R_i has exactly two k-adjacent cells in A.*

As shown in Fig. 2, the meaningful boxes (denoted afterwards by the set $\mathcal{M}$) overlap and thus cannot be viewed as an irregular isothetic object directly (Definition 1). However each one contains a given number of pixels (at the initial resolution) so that the set of boxes $\mathcal{M}$ covers a subset of the input image. This subset $\mathcal{P}$, which is an irregular isothetic object, is transformed into k-arcs, *i.e.* open k-curves, and the respective adjacencies relations between arcs is represented by a Reeb graph structure [22], as illustrated in Fig. 3a [21,23]. In that graph, each edge is associated to an irregular k-arc reconstructed. This process is driven by considering a given order relation, along X or Y axis (in this figure, X axis has been chosen). With the support of the Reeb graph, we are then able to produce a cyclic representation of the contour by parsing k-arcs in a given order (*e.g.* clock-wise from the top-most element). We also remove extra branches of

the graph, *i.e.* edges corresponding to k-arcs not belonging to the cycle (associated to red parts in Fig. 3a). In particular, graph edges comporting a node of degree 1 are removed. At the end of this process, we obtain a single k-curve (Fig. 3b), associated to a cyclic graph, and we consider the interface (Euclidean segment shared) between two consecutive cells in the k-curve, *i.e.* 1-D intervals.

By combining the intervals computed from both X and Y axes, we have thus two lists of segments representing the input contour, denoted by $\mathcal{S}_X$ and $\mathcal{S}_Y$, as shown in Fig. 4a. We set the internal and external points of these straight segments (black and white points in Fig. 4b) by considering the barycenter of the global shape as we did in [21].

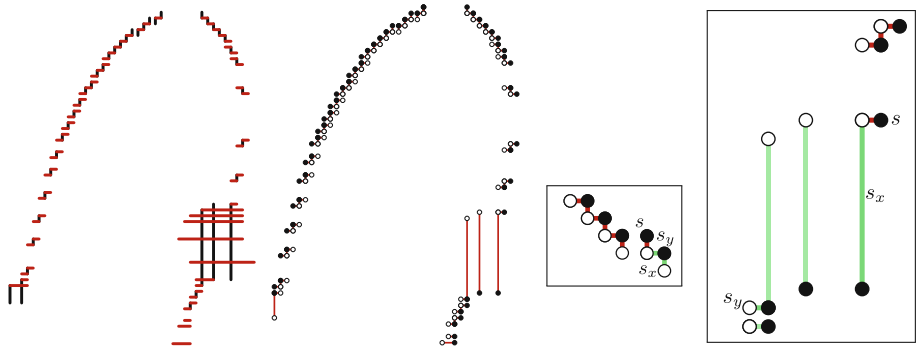

Fig. 4. A part of the two sets $\mathcal{S}_X$ (black) and $\mathcal{S}_Y$ (red) intervals from the *Flower* sample (a), and converted into a single set of intervals $\mathcal{S}_{XY}$ (b). Internal points are dotted in white, external ones in black. We also illustrate some cases of our process, with specific examples of segments s, s_x and s_y (see text) in (c) and (d). In the images, red intervals are already in place in $\mathcal{S}_{XY}$ and green ones are to be processed from $\mathcal{S}_X$, $\mathcal{S}_Y$ (Color figure online)

We then build a single list of intervals $\mathcal{S}_{XY} = \{\mathcal{S}_{XY}[i]\}_{1 \leq i \leq n}$ with X- and Y-aligned elements by first removing segments from $\mathcal{S}_Y$ intersecting one or several ones in $\mathcal{S}_X$ (see again Fig. 4a and b). The converse choice can done (*i.e.* removing segments from $\mathcal{S}_X$ overlapping some of $\mathcal{S}_Y$), nevertheless, our option leads to a faithful representation of the input contour, as exposed later in experiments.

Then, we simultaneously parse the sets $\mathcal{S}_X$ and $\mathcal{S}_Y$ to construct this list by a linear and incremental approach, according to the size of these two lists. At an iteration of this process, consider the last segment added in $\mathcal{S}_{XY}$, denoted by s, and the next segments to be added from $\mathcal{S}_X$ and $\mathcal{S}_Y$, denoted by s_x and s_y respectively. We add in $\mathcal{S}_{XY}$ the closest interval from s. As an illustration, in Fig. 4c, we add s_y, and in Fig. 4d, s_x.

During this process, adding segments of $\mathcal{S}_X$ and $\mathcal{S}_Y$ in $\mathcal{S}_{XY}$ is realized in in $\mathcal{O}(|\mathcal{S}_X| + |\mathcal{S}_Y|)$. We can observe that we build a valid list of segments in $\mathcal{S}_{XY}$,

since two successive segments in the final list (not sharing the same end point) respect this condition:

$$\overrightarrow{\mathcal{S}_{XY}[i]}.\overrightarrow{\mathcal{S}_{XY}\big[(i+1)\bmod n\big]} \geq 0,\ \forall i = 1,\ldots,n, \tag{1}$$

wherein each segment is considered as a vector with the orientation given by internal and external endpoints. For instance, in Fig. 4c, $\overrightarrow{s}.\overrightarrow{s_y} = 0$ and are added successively in $\mathcal{S}_{XY}$, in Fig. 4d, $\overrightarrow{s}.\overrightarrow{s_x} = 0$, and any two consecutive parallel segments $\mathcal{S}_{XY}[i]$ and $\mathcal{S}_{XY}[i+1]$ will respect a strict positive dot product in Eq. 1. The validity of the list $\mathcal{S}_{XY}$ also means that the list of internal points are ordered in the clockwise order, and follow the curvilinear abscissa of the input contour (and this is the same for the list of external points).

4 Recognition of Straight Segments and Circular Arcs

Even if the arrangement of straight segments in $\mathcal{S}_{XY}$ is not completely random, it lacks regularity. For instance, the X-coordinates of the endpoints do not necessarily increase and for this reason, we cannot use the algorithm of O'Rourke [17] for the recognition of straight segments.

In this work, you use a general algorithm for the recognition of both straight segments and circular arcs, formulated as two instances of a *Generalized Linear Programming* (GLP) problem [1].

Our notations and definitions follow [1]. A GLP problem is a family H of constraints and an objective function ω from subfamilies of H to some totally ordered set S. In addition, H and ω must be such that:

(C1) *Monotonicity*: $\forall F \subseteq G \subseteq H,\ \omega(F) \leq \omega(G)$,

(C2) *Locality*: $\forall F \subseteq G \subseteq H$ s.t. $\omega(F) = \omega(G)$ and for each $h \in H$: $\omega(F \cup h) > \omega(F)$ iff $\omega(G \cup h) > \omega(G)$.

Note that the set S must contain a special maximal element Ω so that $G \subseteq H$ is *unfeasible* if $\omega(G) = \Omega$ and *feasible* otherwise.

In our framework, the constraint set H is given by the endpoints of the set of the n straight segments of $\mathcal{S}_{XY}$, with $n \geq 1$. Each straight segment has two endpoints: one with label "white", the other with label "black", as depicted in Fig. 4b. Let us denote the set of white (resp. black) endpoints by $P^\circ := \{p_i^\circ\}_{i=1\ldots n}$ (resp. $P^\bullet := \{p_i^\bullet\}_{i=1\ldots n}$). Let $\mathbb{P}$ (resp. $\mathbb{D}$) be the set of all possible half-planes (resp. disks). For a given $\mathbb{X} \in \{\mathbb{P}, \mathbb{D}\}$, we want to find a shape $X \in \mathbb{X}$ that contains one point set, *e.g.* P°, but not the other. In other words, we want to find $X \in \mathbb{X}$ under the constraint set $H := \{h_{2i-1}, h_{2i}\}_{i=1\ldots n}$, where

$$\forall i = 1,\ldots,n,\ h_{2i-1} := p_i^\bullet \in X,\ h_{2i} := p_i^\circ \notin X. \tag{2}$$

The problem is unfeasible if it does not exist such a X, but feasible otherwise. In the latter case, we search for X minimizing a given objective function.

For any $\mathbb{X} \in \{\mathbb{P}, \mathbb{D}\}$, there exists an objective function $\omega_{\mathbb{X}}$ so that (C1) and (C2) are true, which means that the above problem reduces to a GLP problem.

The objective function $\omega_{\mathbb{D}}$ is chosen to either return Ω if the problem is unfeasible or the radius of a smallest separating disk for H otherwise. By definition, the pair $(H, \omega_{\mathbb{D}})$ satisfies the monotonicity condition (C1), which coarsely says that the larger the constraint set is, the larger the smallest separating disk for this set is. In addition, since $n \geq 1$, the smallest separating disk, if it exists, is unique, which implies locality (C2).

The objective function $\omega_{\mathbb{P}}$ returns Ω if the problem is unfeasible. Otherwise, the convex hulls of the point set to enclose and the point set to not enclose are well-defined because $n \geq 1$ and do not intersect. In this case, $\omega_{\mathbb{P}}$ returns the inverse of the minimal distance between the two convex hulls. The inverse is taken so that adding a non-redundant constraint makes the objective function increase. Again, the pair $(H, \omega_{\mathbb{P}})$ satisfies conditions (C1) and (C2). As a result, depending on $\omega_{\mathbb{X}}$, we have to solve two different kinds of GLP problem.

There exists an easy-to-implement and randomized algorithm that solves these two kinds of GLP problem in expected linear-time [20]. It comes from the well-known randomized algorithm for the smallest enclosing circle problem [25]. It takes a pair $(H, \omega_{\mathbb{X}})$ and returns a basis, i.e. a minimal subfamily $B \in H$ such that $\omega_{\mathbb{X}}(B) = \omega_{\mathbb{X}}(H)$. The combinatorial dimension d of the problem is the maximum size of any basis for any feasible family. For instance, $d = 3$ for $\omega_{\mathbb{D}}$ (resp. $\omega_{\mathbb{P}}$) because at most three constraints uniquely define a disk (resp. the width between two convex polygons).

The algorithm is incremental and recursive. It may be coarsely described as follows. We iteratively add constraints. For each constraint, we check whether the new constraint violates the current basis or not. If yes, then we try to update the basis from the new constraint by recursively calling the same algorithm with all the previous constraints.

It is useful to have an on-line algorithm in order to compute the whole set of maximal segments [7] or arcs [19]. Since the original algorithm [20] is incremental, adding the constraints in order straightforwardly leads to an on-line algorithm. The drawback is that the random order can be used only in the recursive calls but not during the constraint discovery, which results to an increase of the expected time-complexity from linear to quadratic. However, we experimentally observe short running times. The next section shows results of our pipeline, employing this on-line algorithm for the reconstruction of maximal segments or arcs.

5 Experimental Results

We first present in Fig. 5 the whole set of maximal segments and arcs for the *Flower* image. Contrary to the previous work dedicated to pure vectorization [23], we do not calculate a unique polyline from a complex structure of k-arcs. Thanks to the cyclic irregular representation of the input contour, we are capable of reconstructing maximal primitives, bounded by 1-D intervals, whose lengths only depend on local input noise. Without any parameter, we obtain faithful representations of noisy shapes. Moreover, the results do not depend on any starting point, as it could be the case for other methodologies employing

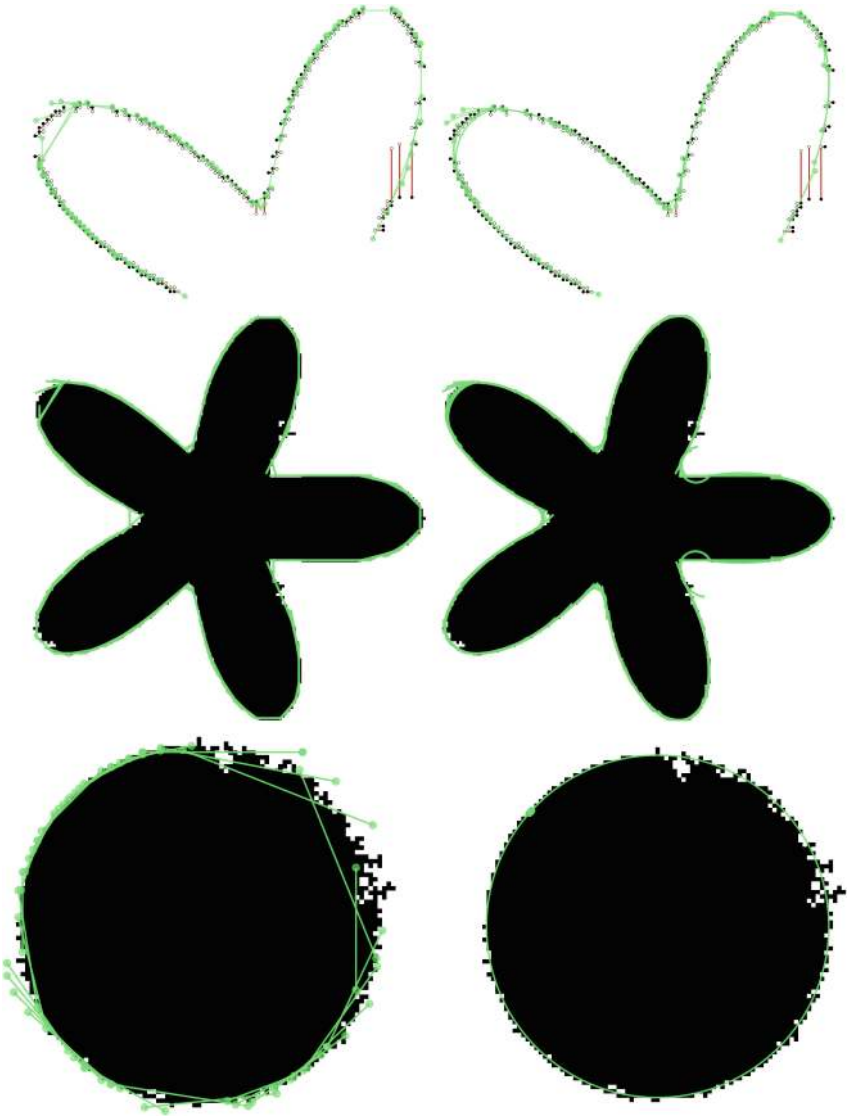

(a) Maximal straight segments (b) Maximal circular arcs

Fig. 5. Top: Decomposition into maximal segments (a) and maximal arcs (b) in a part of the *Flower* sample (green primitives), superimposed on input intervals (presented as in Fig. 4). Center and bottom: The maximal primitives are shown over original digital contour of *Flower* and *Circle* (Color figure online)

greedy algorithms. Even in the case of an high amount of local noise, our algorithm successfully reconstructs sets of primitives, as illustrated in Fig. 5 (bottom) wherein the input digital contour is significantly corrupted and contains large discontinuities and holes (top-right of the shape). As in [21], we can also obtain the circle passing through the contour, by choosing maximal arcs (Fig. 5b).

We finally present the meaningful representation, and sets of maximal straight segments and circular arcs obtained with our algorithm, for two real images, in Fig. 6 (one contour) and Fig. 7 (two contours). The *Char* image leads to a noisy contour (Fig. 6b), which is accurately represented thanks to our algorithm. Maximal primitives (Fig. 6e, f) represent the complete contour, while one of our previous contributions (d) [23], an accurate vectorization by MLP (or Minimum Length Polyline), misses a part of the object, and produces abrupt angles in round parts. The *Sign* image (350 × 350 pixels) allows us to test the scalability of our method. The contours we have extracted generate a high number of meaningful boxes (1,364 boxes for external part, 1,234 for internal part) that we have processed without any extra effort.

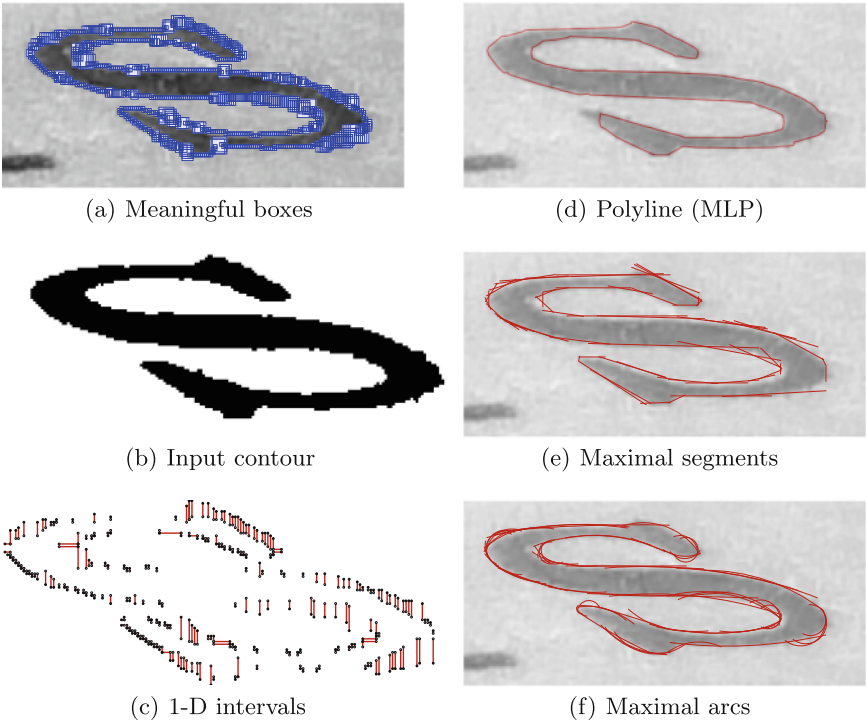

(a) Meaningful boxes (d) Polyline (MLP)

(b) Input contour (e) Maximal segments

(c) 1-D intervals (f) Maximal arcs

Fig. 6. Results of our algorithm with the real image *Char* of size 185 × 85 pixels

(a) Meaningful boxes (b) Maximal segments (c) Maximal circular arcs

Fig. 7. Results of our algorithm with the real image *Sign* of size 350 × 350 pixels

6 Conclusion and Future Works

In this article, we have proposed a novel approach combining multi-scale and irregular isothetic representations for the geometrical reconstruction of digital noisy contours. Our algorithm calculates a set of 1-D bounding intervals of the input shape, which permits to apply an on-line and incremental recognition algorithm. Our contribution has been successfully applied on synthetic and real images, encouraging us to exploit it in concrete image analysis contexts, and to investigate several lines of research.

Our first concern will consists in adapting the tangential cover approach [6] to our cyclic irregular representation. This will enable the calculation of a structure containing successive primitives, instead of overlapping maximal segments or arcs. Second, we would like to compare our contribution with other methods selected from state-of-the-art, *e.g.* [15,16], and to test their robustness [24] with challenging data-sets of binary shapes, such as KIMIA. As a longer term, we plan to investigate the more general question of reconstructing digital shapes with other geometrical primitives, like B-splines and other parametric curves, with a similar framework we have presented herein.

References

1. Amenta, N.: Helly-type theorems and generalized linear programming. Discrete Comput. Geom. **12**(3), 241–261 (1994)
2. Atallah, M.J., et al.: An optimal algorithm for shortest paths on weighted interval and circular-arc graphs. Appl. Algorithmica **14**(5), 429–441 (1995)
3. H.S., B.: Structured Document Image Analysis. Springer, Heidelberg (1992). doi:10.1007/978-3-642-77281-8
4. Bo, P., et al.: A graph-based method for fitting planar b-spline curves with intersections. J. Comput. Des. Eng. **3**(1), 14–23 (2016)
5. Faure, A., Feschet, F.: Multi-primitive analysis of digital curves. In: Wiederhold, P., Barneva, R.P. (eds.) IWCIA 2009. LNCS, vol. 5852, pp. 30–42. Springer, Heidelberg (2009). doi:10.1007/978-3-642-10210-3_3

6. Feschet, F., Tougne, L.: On the min DSS problem of closed discrete curves. Discrete Appl. Math. **151**(1–3), 138–153 (2005)
7. Feschet, F., Tougne, L.: Optimal time computation of the tangent of a discrete curve: application to the curvature. In: Bertrand, G., Couprie, M., Perroton, L. (eds.) DGCI 1999. LNCS, vol. 1568, pp. 31–40. Springer, Heidelberg (1999). doi:10.1007/3-540-49126-0_3
8. Goshtasby, A.A.: Fitting parametric curves to dense and noisy points. In: International Conference on Curves and Surfaces (1999)
9. Hilaire, X., Tombre, K.: Robust and accurate vectorization of line drawings. IEEE Trans. Pattern Anal. Mach. Intell **28**(6), 890–904 (2006)
10. Karasalo, M., et al.: Contour reconstruction using recursive smoothing splines - algorithms and experimental validation. Robot. Auton. Syst. **57**(6–7), 617–628 (2009)
11. Kerautret, B., Lachaud, J.O.: Meaningful scales detection along digital contours for unsupervised local noise estimation. IEEE Trans. Pattern Anal. Mach. Intell. **34**(12), 2379–2392 (2012)
12. Kerautret, B., Lachaud, J.O.: Meaningful scales detection: an unsupervised noise detection algorithm for digital contours. Image Process. On Line **4**, 98–115 (2014)
13. Lachaud, J.O., Non-Euclidiens, E., d'Image, A.: Modèles Déformables Riemanniens et Discrets, Topologie et Géométrie Discrète. Habilitation à Diriger des Recherches, Université Bordeaux 1 (2006). (en francais)
14. Lebrun, M., et al.: Secrets of image denoising cuisine. Acta Numer. **21**, 475–576 (2012)
15. Ngo, P., Nasser, H., Debled-Rennesson, I., Kerautret, B.: Adaptive tangential cover for noisy digital contours. In: Normand, N., Guédon, J., Autrusseau, F. (eds.) DGCI 2016. LNCS, vol. 9647, pp. 439–451. Springer, Cham (2016). doi:10.1007/978-3-319-32360-2_34
16. Nguyen, T.P., Debled-Rennesson, I.: Decomposition of a curve into arcs and line segments based on dominant point detection. In: Heyden, A., Kahl, F. (eds.) SCIA 2011. LNCS, vol. 6688, pp. 794–805. Springer, Heidelberg (2011). doi:10.1007/978-3-642-21227-7_74
17. O'Rourke, J.: An on-line algorithm for fitting straight lines between data ranges. Commun. ACM **24**(9), 574–578 (1981)
18. Rosin, P.L., West, G.A.W.: Nonparametric segmentation of curves into various representations. IEEE Trans. Pattern Anal. Mach. Intell. **17**(12), 1140–1153 (1995)
19. Roussillon, T., Lachaud, J.-O.: Accurate curvature estimation along digital contours with maximal digital circular arcs. In: Aggarwal, J.K., Barneva, R.P., Brimkov, V.E., Koroutchev, K.N., Korutcheva, E.R. (eds.) IWCIA 2011. LNCS, vol. 6636, pp. 43–55. Springer, Heidelberg (2011). doi:10.1007/978-3-642-21073-0_7
20. Sharir, M., Welzl, E.: A combinatorial bound for linear programming and related problems. In: Finkel, A., Jantzen, M. (eds.) STACS 1992. LNCS, vol. 577, pp. 567–579. Springer, Heidelberg (1992). doi:10.1007/3-540-55210-3_213
21. Toutant, J.-L., Vacavant, A., Kerautret, B.: Arc recognition on irregular isothetic grids and its application to reconstruction of noisy digital contours. In: Gonzalez-Diaz, R., Jimenez, M.-J., Medrano, B. (eds.) DGCI 2013. LNCS, vol. 7749, pp. 265–276. Springer, Heidelberg (2013). doi:10.1007/978-3-642-37067-0_23
22. Vacavant, A., Coeurjolly, D., Tougne, L.: Topological and geometrical reconstruction of complex objects on irregular isothetic grids. In: Kuba, A., Nyúl, L.G., Palágyi, K. (eds.) DGCI 2006. LNCS, vol. 4245, pp. E1–E1. Springer, Heidelberg (2006). doi:10.1007/11907350_58

23. Vacavant, A., et al.: A combined multi-scale/irregular algorithm for the vectorization of noisy digital contours. Comput. Vis. Image Underst. **117**(4), 438–450 (2013)
24. Vacavant, A.: A novel definition of robustness for image processing algorithms. In: Kerautret, B., Colom, M., Monasse, P. (eds.) RRPR 2016. LNCS, vol. 10214, pp. 75–87. Springer, Cham (2017). doi:10.1007/978-3-319-56414-2_6
25. Welzl, E.: Smallest enclosing disks (balls and ellipsoids). In: Maurer, H. (ed.) New Results and New Trends in Computer Science. LNCS, vol. 555, pp. 359–370. Springer, Heidelberg (1991). doi:10.1007/BFb0038202
26. Wirjadi, O.: Survey of 3D image segmentation methods. Berichte des Fraunhofer ITWM, p. 23 (2007)